

Chapter 1

Three-Dimensional Printing of Nanocellulose-Based Hydrogels



Sahar Sultan and Aji P. Mathew

Abstract This chapter gives an overview of the recent developments in the field of three-dimensional (3D) printing of nanocellulose-based hydrogels. Nanocellulose has gained much attention due to its renewable sources, low toxicity, biocompatibility, good mechanical properties and availability of surface charges for further modifications as well as in situ growth of functional nanoparticles. Moreover, suitable rheological properties of nanocellulose are helpful in utilizing 3D printing technique for producing constructs with customized, controlled and complex geometries. This technique offers a high-resolution 3D constructs with precise micro- and macroscaled structures and can be extended to 3D bioprinting, where living cells are mixed in hydrogel inks. As the name suggests, nanocellulose-based hydrogel inks contain nanocellulose as reinforcement phase, while other crosslinkable biopolymers can serve as matrix phase.

1 Background

Keeping in mind the depletion of petroleum-based resources and environmental issues, cellulose is a good choice of materials for future because of its renewability, biodegradability and environmental friendliness. Cellulose is the most abundant natural biopolymer on Earth with an annual production of 10^{10} – 10^{11} tons [1]. It has a variety of sources and can be extracted from a top-down approach from marine animals (e.g., tunicates) and plants (e.g., wood, cotton, wheat straw). It can also be obtained via bottom-up approach through biosynthesis such as bacteria (*Acetobacter Xylinum*), algae (e.g., *Valonia*), fungi and even amoeba (protozoa) [2]. Cellulose is a long-chain polysaccharide having a chemical formula of $(C_6H_{10}O_5)_n$ where n is the degree of polymerization depending on the sources and pretreatments of cellulose. It consists of linear chain of glucose units linked via a β -1,4 glycosidic bond [3].

S. Sultan (✉) · A. P. Mathew
Department of Materials and Environmental Chemistry, Stockholm University, Stockholm, Sweden
e-mail: sahar.sultan@mmk.su.se

Cellulose with at least one dimension on a nanoscale (1–100 nm) is termed as nanocellulose and can be isolated from cellulose biomass following a top-down approach (Fig. 1). Nanocellulose not only possesses the properties of cellulose, such as mechanical strength, potential for chemical modification, low toxicity, biocompatibility, biodegradable and renewability, but it also has nanoscale characteristics like high specific surface area, rheological and optical properties [4]. The family of nanocellulose is divided into three types: (i) cellulose nanofibers (CNF), (ii) cellulose nanocrystals (CNC) and bacterial cellulose (BC) (Table 1).

CNF consists of both individual and aggregated nanofibers including ordered and disordered regions, which attribute the morphology of CNF with soft and long chains [6]. For the production of CNF, mainly, mechanically induced destruction strategy is used followed by homogenization at high pressure. In this process, the individual microfibrils are delaminated from cellulosic fibers by multiple mechanical shearing actions that require high energy consumptions [7]. However, different pretreatments of cellulosic fibers can facilitate the delamination process, e.g., alkali, oxidative, enzymatic and acidic pretreatments. Alkali pretreatment removes a certain amount of lignin that interrupts its structure and weakens the bonds between lignin and carbohydrates [8]. 2,2,6,6-tetramethylpiperidine-1-oxyl radical (TEMPO)-mediated oxidation of native celluloses is also a pretreatment used for conversion of hydroxyl groups to carboxylate groups [9]. This surface treatment induces a negative charge

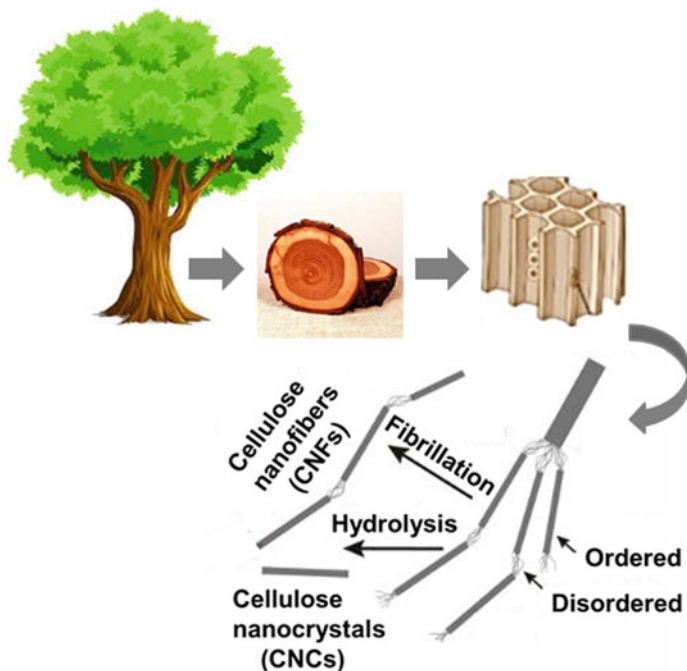
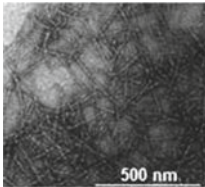
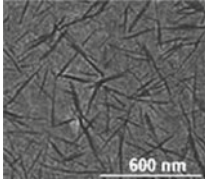
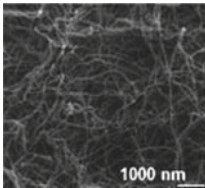


Fig. 1 Top-down approach for the production of plant-derived nanocellulose

Table 1 Family of nanocellulose [2, 5]

Types of nanocellulose	Synonyms	Typical sources	Formation and average size
Cellulose nanofibrils (CNF) 	Microfibrillated cellulose, nanofibrils and microfibrils, nanofibrillated cellulose	Wood, sugar beet, potato tuber, hemp, flax	<ul style="list-style-type: none"> – Delamination of woodpulp by mechanical pressure before and/or after chemical or enzymatic treatment – Diameter: 5–60 nm – Length: several micrometers
Cellulose nanocrystals (CNC) 	Nanocrystalline cellulose, crystallites, whiskers, rodlike Cellulose microcrystals	Wood, cotton, hemp, flax, wheat straw, mulberry bark, ramie, Avicel, tunicin, cellulose from algae and bacteria	<ul style="list-style-type: none"> – Acid hydrolysis of cellulose from many sources – Diameter: 5–70 nm – Length: 100–250 nm (from plant celluloses); 100 nm to several micrometers (from celluloses of tunicates, algae, bacteria)
Bacterial cellulose (BC) 	Bacterial cellulose, microbial cellulose, biocellulose	Low-molecular-weight sugars and alcohols	<ul style="list-style-type: none"> – Bacterial synthesis – Diameter: 20–100 nm – Different types of nanofiber networks

resulting in repulsion between cellulosic fibers, thus facilitating fibrillation process. In addition, these carboxylate group can be used for further surface attachment of other functional molecules [10]. TEMPO-CNF (TOCNF) can also be produced directly from bagasse, which is an agro-industrial residue [11]. Enzymes show strong synergistic effects to facilitate disintegration of cellulosic fibers [12]. CNF produced from enzymatically pretreated cellulosic wood fibers showed certain improvements as compared to acidic pretreatment [13], which decreases the chain length of the cellulose molecule causing embrittlement [14].

The disordered regions in the cellulosic fibers can be removed by a strong acid hydrolysis treatment resulting in crystalline rod-shaped CNCs. During this process, the hydronium ions penetrate the amorphous regions of cellulose chains, promoting the hydrolytic cleavage of the glycosidic bonds and releasing individual crystallites [15]. The commonly acid used is sulfuric acid as its reaction with the surface hydroxyl

groups via an esterification process allows the grafting of anionic sulfate ester groups [16]. These negatively charged groups induce the formation of an electrostatic layer covering the nanocrystals and promote their dispersion in water [15].

During the biosynthesis of BC, the glucose chains are produced inside the bacterial body that are extruded out through pores present on the cell envelope [6]. The combination of these chains produces microfibrils that further aggregates as ribbons and generates a web-shaped network structure with BC [17]. BC has certain advantages as compared to CNF and CNC, such as better mechanical and chemical properties, high crystallinity as well as purity and control over its repeating unit and the molecular weight based on fermentation process [18, 19]. However, the relatively high cost associated with the support the growth of bacteria and low yield has limited its use if any mass production is to be considered.

2 Introduction

The research and development on the manufacturing processes to make nanocellulose into useful forms is an essential part of the development of cellulose nanocomposites. To produce cellulose nanocomposites for commercial use, the journey from laboratory to industry must contain such methods, reagents, solvents, equipments that have the potential for large-scale production.

The structure and properties of cellulose nanocomposites rely on the fiber–fiber bonding as well as fiber–matrix interfacial adhesion, which in return are dependent on the homogeneity of the nanocellulose dispersion in the matrix phase [20]. The hydrophilic nature and low thermal stability of nanocellulose limit the choice of matrix and processing techniques to form composites. The abundance of hydroxyl groups at the surface of nanocellulose makes surface functionalization possible that plays an important role to increase the surface hydrophobicity while maintaining the thermal stability [20]. The main idea behind surface functionalization is to obtain better dispersion through the introduction of stable negative or positive electrostatic charges and to tune the surface energy characteristics to improve compatibility with matrices in nanocomposites [21]. Furthermore, cationic or anionic surface charges can be incorporated, which can later be used for in situ growth of other functional molecules [22, 23].

The commonly used traditional methods for the production of cellulose nanocomposite are casting, extrusion, electrospinning and freeze-drying. The earlier publications dealing with cellulose-reinforced nanocomposites were based on casting/evaporation of an aqueous mixture of CNCs [24–26]. Nowadays, the use of the casting/evaporation technique is not limited to a water medium but is extended to organic solvents, e.g., dimethylformamide [27], pyridine [28], toluene [29] and chloroform [30]. Electrospinning is relatively a new technique and has the ability to

produce three-dimensional (3D) cellulose nanocomposites with very high surface-area-to-volume ratio [31] and enhanced mechanical properties together with its electrical conductivity [22, 32]. In addition, the high surface area and microporous structure of electrospun fiber mats can absorb wound exudates, prevent excess dehydration and microbial infection as well as facilitate gas permeability. These properties make them suitable for cell attachment and proliferation in wound dressing applications [33, 34]. Freeze-drying also known as ice crystal templating offers an advantage of designing hierarchically structured composite materials by controlling the rate and direction of freezing ice [35]. CNF- and CNC-based composites can be fabricated via freeze-drying technique to have 3D scaffolds or 2D membranes [36, 37]. Another fabrication technique is melt processing in which cellulose nanomaterials are dispersed in a thermoplastic polymer melt. The first study on nanocellulose melt process reported nanocomposites developed by melt extrusion technique using a commercially available grade of microcrystalline cellulose in a biodegradable polyester matrix [38]. Later studies used polyethylene [39] and polyoxyethylene [40] as polymer matrices. However, these traditional techniques do not enable precise control of internal scaffold architecture or the fabrication of complex architectures. Moreover, they also require good fabrication skills to maintain consistency and reproducibility in the scaffold architecture.

Recently, three-dimensional (3D) printing technique has been adapted for the fabrication of 3D constructs based on the digitally controlled deposition of successive layers of material until a final structure is created with precise geometric control at macro- and microscale [41]. The process of 3D printing starts with a computer-aided design (CAD) file that can be obtained by a 3D scanner or by means of photogrammetry where the model is obtained through the combination of several images of the object taken from different positions [42]. This is an advantage in biomedical field where computed tomography (CT) or magnetic resonance imaging (MRI) of the patient can be used to create customized 3D-printed models (Fig. 2b) [43]. Currently, 3D printing techniques are classified into extrusion, powder-based, photopolymerization and lamination [42].

In case of hydrogel or paste, extrusion-based 3D printing is a popular choice as the “ink” is in a highly viscous liquid state, which is able to retain its shape after deposition (Fig. 2a) [42]. The freestanding 3D objects can be crosslinked during or after the 3D printing via ultraviolet (UV) curing or ionic crosslinking [44, 45]. However, to print hydrogel inks with high resolution is a challenge due to the swelling that occurs when viscous liquefied material is extruded through a small nozzle with high pressures. As a potential candidate for 3D printing, the rheological properties of the hydrogel ink are of prime importance. The hydrogel should have strong non-Newtonian shear thinning behavior along with viscoelastic solid-like response [44]. During extrusion, the viscosity of the hydrogel drops due to higher shear rates, but as soon as the hydrogel is extruded and shear rate drops, the viscosity of the ink increases immediately. 50 s^{-1} is a typical shear rate experienced during 3D printing [46]. This shear thinning property is an important factor to make filamentary extrusion possible. To maintain the shape of the construct after 3D printing, the hydrogel should have

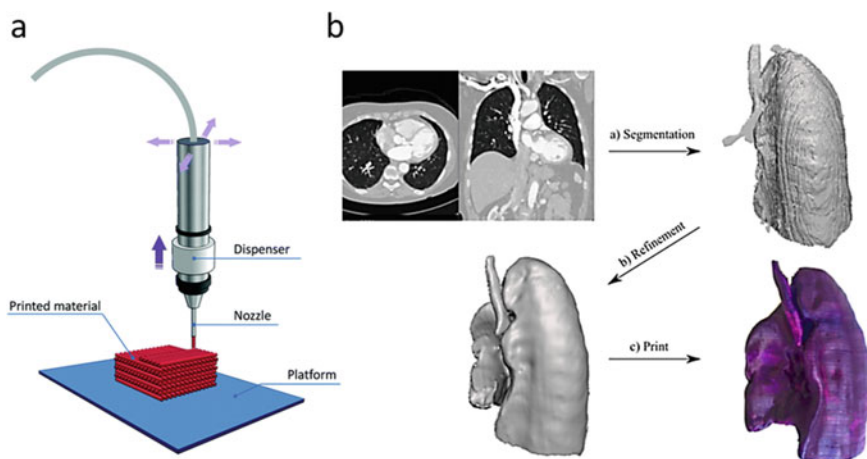


Fig. 2 a Schematic representation of extrusion-based 3D printing for ink and b work flow from medical imaging data (CT scan) to a finished 3D-printed model

a storage modulus (G') sufficiently higher than its loss modulus (G''). This solid-like behavior of the hydrogel is highly desirable for subsequent post-treatments and handling [47].

An advancement of 3D printing is 3D bioprinting, where both living and non-living biological materials are used to fabricate 3D scaffolds, implants, engineered tissues and organs [48]. A construct is said to be 3D bioprinted when living cells, bioactive molecules, growth factors, biomaterials or cell-aggregates are mixed with the hydrogel ink or are incorporated through a separate nozzle [49]. In this way, the rejection rate of foreign objects by the human body is reduced and recovery rate is accelerated. However, extra care has to be taken when dealing with 3D printing of bioinks. Physically, the bioink should be sufficiently viscous to be dispensed as a free-standing filament but too high concentration of the bioink can negatively affect cell viability [50]. Factors such as too strong shear forces required to eject the bioink, high printing temperatures and harsh post-treatments can result in cell death. One study demonstrated an inverse relationship between extrusion pressure and cellular viability [51]. The study reveals that the high dispensing pressure and small nozzle size induce mechanical damage to cell membrane integrity causing loss in cell viability.

3 3D Printing of Nanocellulose-Based Hydrogels

The surface charges and water stability of nanocellulose allow forming hydrogels from a nanocellulose solution through physical crosslinking with inherent shear thinning property [52]. Hydrogel formation capability of nanocellulose at low concentrations (1–2 wt%) has facilitated the use of 3D printing as a fabrication technique for 2D and 3D scaffolds [53, 54]. The presence of nanocellulose is expected to enhance the elastic modulus of the nanocomposite hydrogel ink that prevents the flow and deformation of the deposited material as the shear force ceases after extrusion [47]. The presence of stiff reinforcement particles such as CNCs can introduce shear-induced alignment that is considered beneficial for inducing directionality in the 3D constructs [45]. The local orientation control of CNFs can define the elastic and swelling anisotropies for biomimetic 4D printing [55]. As compared to CNCs, CNFs readily form hydrogels at low concentration due to its long and entangled chain network. In contrast, CNCs can produce concentrated hydrogels at a given viscosity due to lower aspect ratio of CNCs than CNFs [56].

The 3D-printed structures must have fast crosslinking abilities for post-processing, handling and retaining its structure after printing. The surface charges present on nanocellulose surface can be utilized for its self-crosslinking functionalization, i.e., without the need for a matrix phase [57] or the 3D-printed constructs can directly be freeze-dried to form aerogels [58]. However, in most case alginate is a popular choice to be used as a crosslinkable matrix phase because of its bio-based origin, relatively low cost and ability of fast gelation in the presence of divalent cations [59]. In case of biomedical applications, alginate alone has low cell adhesion and cell proliferation capability, and therefore, it is often mixed with other biopolymers, such as gelatin [44]. The blends of alginate and gelatin are used to print 3D constructs for myoregenerative applications [50] or to fabricate living heterogeneous aortic valve conduits [60].

3.1 CNF-Based Hydrogels

Highlight	Composition	Post-treatment	Application	References
Human stem cell-decorated CNF threads	CNF: 1.47 (wt%)	Glutaraldehyde crosslinking	Wound dressing	[61]
Commercially available ink CELLINK	CNF/alginate 2.0/0.5 (wt%)	CaCl ₂ crosslinking	Auricular cartilage regeneration	[62–64]
3D bioprinting human chondrocytes	CNF/alginate 2.0/0.5 (wt%)	CaCl ₂ crosslinking	Cartilage tissue engineering	[64, 65]
Solidification of cellulose nanofibril hydrogel into controlled 3D architectures	CNF 2 wt% CNF/carbon nanotubes 2/0.2 (wt%)	CaCl ₂ crosslinking followed by air drying/air drying with surfactants/solvent exchange/freeze drying Air drying	Diverse	[66]
Bioink: C- periodate nanocellulose substrate: TOCNF	CNF 3.9 wt%	CaCl ₂ crosslinking followed by freeze-drying	Wound dressing	[67]
3D bioprinting of induced pluripotent stem cells (iPSCs)	CNF/alginate 60/40 (dry wt%) + iPSCs CNF/hyaluronic acid 95/5 (% volume) + iPSCs	CaCl ₂ crosslinking H ₂ O ₂ crosslinking	Cartilage tissue engineering	[68]
Bioink with functionalized matrix	Alginate sulfate/nanocellulose 1/1.36 (%) + Passage 3 cells	CaCl ₂ crosslinking	Cartilage Bioprinting	[69]
Biomimetic inks based on tyramine-functionalized xylan (XT)	CNF/XT 2.6–3.0/5.11–5.8 (wt%)	H ₂ O ₂ crosslinking	Diverse	[70]
Biofunctionalization: conjugation of avidin to TOCNF hydrogel	Alginate/TOCNF 90/10 (wt%) + Water/glycerin 45/50 (v%)	CaCl ₂ crosslinking	Biomedical devices and drug-releasing	[71]
CNF tubes as sacrificial templates	TOCNF 1 wt%	Glutaraldehyde and/or CaCl ₂ crosslinking	Biomedical	[72]

(continued)

Highlight	Composition	Post-treatment	Application	References
(continued)				
Composite microfiber based on carbon nanotube/nanofibrillated cellulose	TOCNF/CNT 1/1 (%)	Solvent exchange followed by drying under tension	Flexible electronics	[73]
Blend of CNF and lignosulfonate (LG) for 3D printing and carbonization	CNF/LG 0.25–2/20–50 (wt%)	RT drying/freeze drying followed by carbonization at 800 °C	Energy storage devices	[74]
Biomimetic 4D printing	CNF/clay/monomer/glucose 0.73/9.7/7.8/3.8(%)	Ultraviolet curing	Diverse	[55]
TOCNF aerogel	TOCNF/Kymene 2.8/0.06 (wt%)	Freeze drying followed by crosslinking at 120°	Diverse	[75]
In situ synthesis of Metal organic frameworks onto TOCNF	TOCNF/ZIF-8/Alginate/Curcumin 19.7–66.3/30.8–70.7/2.9–5.5/0–4.1 (%)	CaCl ₂ crosslinking	Biomedical	[10]
Mechanical gradients in nanocellulose papers	TOCNF/copolymer 90–20/10–80	RT drying	Diverse	[76]
Improved rheological properties by the addition of CNF	CNF/GelMA 0–2.0/5.0 (%w/v)	Chemical crosslinking	Biomedical	[53]

Paul Gatenholm initiated the 3D printing of nanocellulose by formulating a bioink with CNF, where alginate was used as matrix [65]. Human chondrocytes in the bioink exhibited a cell viability of 73 and 86% after 1 and 7 days of 3D culture that shows the potential for cartilage tissue engineering applications. The bioink-enabled printing of 2D grid-like structures as well as 3D constructs. He also tested a commercially available ink, CELLINK with 2 wt% CNF for 3D bioprinting [62]. This ink was mixed with primary nasal chondrocytes, which upon 3D printing provides cell-laden, patient-specific auricular constructs with an open inner structure, high cell density, homogenous cell distribution and 3D culture for up to 28 days. These properties combined with 3D printability make this bioink promising for auricular cartilage applications.

Pure CNF extracted from plants can produce crosslinked threads with high mechanical strength for biomedical applications [61]. The threads were decorated with human adipose mesenchymal stem cells (hASC) which is an efficient and safe means to reduce inflammation and promote wound healing. Functionalized CNF can also be used to 3D print constructs. CNF treated with a combination of carboxymethylation and periodate oxidation was used as an ink (3.9 wt%) to 3D print onto TOCNF substrate [67]. The freeze-dried 3D-printed constructs did not support bacterial growth, which can be a distinct advantage for wound dressing applications. TOCNF can be 3D printed where structures collapse upon drying, but by using different drying processes, the collapse can be controlled and the 3D structure can be preserved upon solidification [66]. TOCNF can be used to fabricate highly deformable and shape recoverable 3D-printed aerogels [75]. The surface charges present on CNF participated in crosslinking and allowed freeze-dried TOCNF aerogel to maintain structural integrity even under water and after 80% compression cycles.

The surface charges present on TOCNF can be utilized for in-situ growth of other functional materials after which the hydrogel ink can be utilized for 3D-printing scaffolds (Fig. 3) [10]. The carboxylic groups on TOCNF surface were used for in situ growth of ZIF-8. The inherent porosity of MOF was used to load curcumin, which shows pH-controlled release. This one-pot synthesis method can load up to 70% of MOF particles. The flexibility and extendibility of this system was proved by synthesizing a different MOF, MIL-100, and loading a different guest molecule, methylene blue (MB).

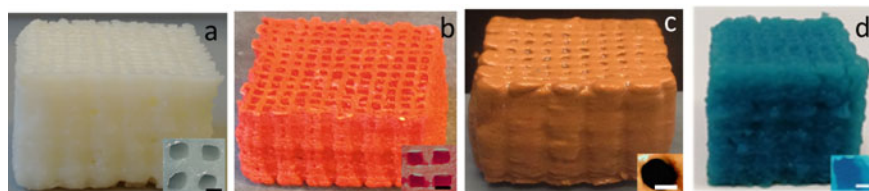


Fig. 3 In situ synthesis of metal organic frameworks onto TOCNF with and without guest molecules **a** ZIF-8@TOCNF, **b** Curcumin-ZIF-8@TOCNF, **c** Curcumin-MIL-100@TOCNF and **d** MB-ZIF-8@TOCNF. Scale bar: 1 mm

In developing cellulose-based hydrogels, instead of nanocellulose, matrix phase can also be functionalized to make its surface suitable for further attachment of growth factors that can induce cell proliferation. Muller and coworkers introduced a sulfated version of alginate, which can bind growth factors such as fibroblast growth factor (FGF), transforming growth factor (TGF) and hepatocyte growth factors (HGF) which induce potent proliferation and collagen II deposition by encapsulated bovine chondrocytes [69]. When this functionalized matrix (1%) was mixed with nanocellulose purchased from CELLINK AB (1.36%) and with passage three cells, a bioink suitable for 3D printing was developed for cartilage applications.

The hydrogel ink can be biofunctionalized by the covalent coupling of an enhanced avidin protein to TOCNF where glycerin was also used as a solvent together with water [71]. Glycerin was used to minimize excess shrinkage that will help 3D-printed samples to retain its dimensions. It was found that the 3D-printed samples without glycerin were not stable at room temperature and had to be freeze-dried; however, in the presence of glycerin, the samples were stable in room temperature after curing.

One step further, 4D biomimetic printing is achieved through the composite ink composed of stiff CNFs embedded in a soft acrylamide matrix, which mimics the composition of plant cell walls [55]. 4D-printing method relies on the ability to define the swelling anisotropies by local control of the orientation of cellulose fibers within the hydrogel composite. During printing, CNF undergoes shear-induced alignment as the hydrogel ink flows through the deposition nozzle, which induces anisotropic stiffness, and, hence, anisotropic swelling along the longitudinal printing direction. This study opens new avenues for creating designer shape-shifting architectures for tissue engineering, biomedical devices, soft robotics and beyond. In another study, TOCNF was used to fabricate a new design approach toward 4D printing, by direct filament writing of CNF-copolymer hydrogels of different composition next to each other in stripe patterns [76]. Subsequent self-healing of the hydrogels during drying leads to coherent films having linear, parabolic and striped bulk gradients leading to optimized combinations of stiffness and toughness.

Carbon nanotubes (CNTs) serve as building blocks to make mechanically robust conductive microfibers owing to their impressive mechanical and electrical properties. Both CNFs and TOCNFs have been used to make hydrogels with CNTs and 3D printed into various constructs [66, 73]. A conductive CNF-CNT hydrogel has been fabricated which demonstrate that the CNF can be functionalized by the addition of conductive CNTs, and the 3D structure can be controlled by the print design and drying mechanism. In case of 3D-printed TOCNF-CNT constructs, both the fibers were aligned in the printing direction due to shear-induced stresses. This alignment helps to improve the interaction and percolation between these two building blocks, leading to a combination of high mechanical strength and electrical conductivity. In addition, microfibrillated cellulose and lignosulfonate hydrogel were fabricated and used to fabricate carbon objects through 3D printing and carbonization [74]. The hydrogel rheological behavior was studied through flow and thixotropic modes which were further used to search for formulation/processability correlations during 3D printing.

Poly(lactic acid) (PLA)-grafted cellulose nanofiber composite filaments were produced by melt extrusion [77]. The grafted PLA was highly crystallized which improved storage modulus of the composite filaments in both low-temperature glassy state and high-temperature rubbery state. Post-extrusion annealing treatment also had a positive effect on the tensile modulus and strength of the composite filaments. The formed composite filaments show potential to be used in 3D printing. In a similar study, polypropylene and CNF nanocomposites were also melt extruded [78].

3.2 BC-Based Hydrogels

Highlight	Composition	Post-treatment	Application	References
Dissolved BC in ionic liquid (IL)	BC: 4 wt%	Solvent exchange followed by freeze drying	regenerated cellulose structures	[79]
3D printing of bacteria	Sodium hyaluronate/fumed silica/carrageenan 1/1/1 (wt ratio) + multifunctional bacteria stem solution Bacteria + Alginate: 2.5 (wt%)	Ultraviolet curing/ Light curing CaCl ₂ crosslinking	biotechnological and biomedical	[80, 81]

BC dissolved in an ionic liquid (1-ethyl-3-methylimidazolium acetate) was used for controlled dispensing, where water and agar aqueous gel were evaluated as coagulating solvents [79]. The highest concentration (4%) of the dissolved BC works best for printing. Water coagulation ensured good resolution but caused complications when multiple layers were extruded on top because of poor adhesion between layers. However, when dissolved BC was dispensed onto an agar gel, the print was coagulated within seconds. The agar gel diffuses through the print from the bottom up, making it possible for the next layer to adhere to the partially gelled first layer. For taller structures, vertical agar supports were used to ensure a constant and continuous coagulation of the 3D prints. This study shows that quality of the 3D-printed constructs is dependent on the needle size, the viscosity of the solution, the pressure during dispensing, and the coagulation method.

A new strategy has been proposed where fully grown bacteria is embedded in a biocompatible ink which is 3D printed to produce bacteria-derived functional materials [80]. Two types of “living materials” were printed which were capable of degrading pollutants and of producing medically relevant bacterial cellulose. Bacterial cellulose films were grown in complex geometries precisely at the site of interest by locally deploying bacteria where needed. This versatile bacteria-printing platform

can be used for the 3D printing of a new generation of biologically generated functional materials. In another study, 2.5 wt% alginate ink was used to deposit bacteria cells in specific three-dimensional patterns to fabricate spatially patterned materials [81].

3.3 CNC-Based Hydrogels

Cellulose nanocrystals are anisotropic particles with a high aspect ratio due to which shear-induced alignment can be expected. Siqueria and coworkers investigated and quantified the shear-induced alignment of anisotropic CNCs during 3D printing [45]. For this purpose, 20 wt% CNC aqueous ink was used which upon drying resulted in printed architectures containing 100% CNC. In the 3D-printed samples, highest degree of orientation (84%) was obtained along the longitudinal direction, i.e., the printing direction (Fig. 4b). In addition, the effect of this alignment on the mechanical properties was studied by developing composite hydrogel inks made from chemically modified CNC for ultraviolet (UV) curing. Interestingly, the mechanical tests reveal enhanced mechanical properties in the longitudinal direction likely arise due to the orientation of the CNCs along the printed filament. In our recent study, we

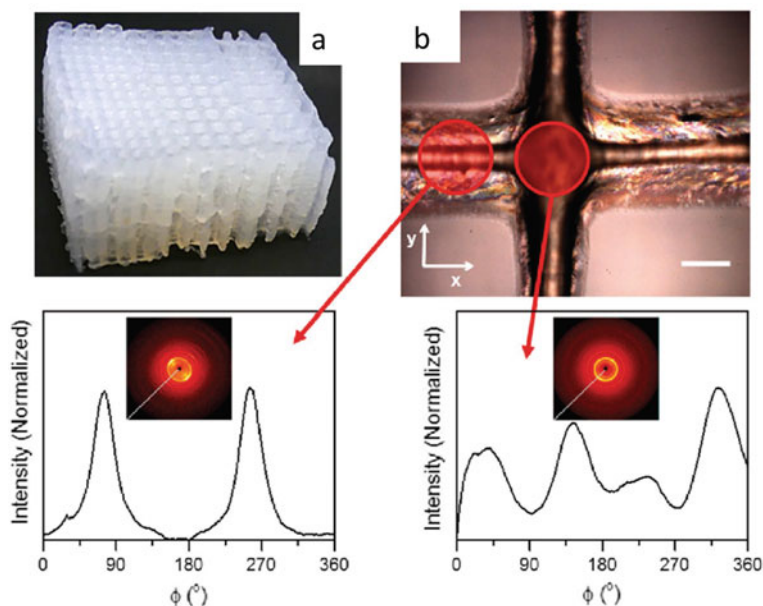


Fig. 4 Optical microscopy images of **a** 3D-printed scaffold with gradient porosity based on CNC hydrogel ink. **b** 3D-printed grids showing the positions for scattering measurements performed along axial or cross-sectional directions

took one step forward and introduced gradient porosity within one hydrogel scaffolds (Fig. 4a) [44]. A variety of 2D and 3D hydrogel scaffolds were produced with uniform and gradient porosity. The 2D wide angle X-ray scattering studies showed that the degree of orientation for CNCs varied between 61 and 76% preferably in the printing direction. This work also highlights the importance of the nozzle movement and printing pathways to obtain 3D hydrogel scaffolds with higher Z-axis while maintaining good resolution.

Pure CNC suspensions have also been used to produce 3D aerogels with controlled structures and inner pore architectures through freeze-drying [58]. An aerogel density range of 127–399 mg/cm³ and a porosity range of 92.1–75.0% were achieved with CNC gel concentrations of 11.8–30 wt%. The preparation and extraction methods of CNCs is also a vital role in its performance and properties. CNCs when prepared through fully recyclable oxalic acid(OA) hydrolysis along with disk-milling (DM) pretreatment of bleached kraft pulp, show several advantages including large aspect ratio, carboxylated surface and excellent thermal stability along with high yield [82]. This CNC suspension was used to produce high-performance films and 3D-printed patterns which can be used for a wide variety of applications. Surface-functionalized CNCs can also be used to produce freestanding 3D-structured objects. A photoactive bis(acyl)phosphaneoxide(BAPO) derivative was directly attached to CNCs without any pretreatment, and these surface-modified CNCs were used for 3D printing [83]. This photoactive nanomaterial can be used to convert a conventional monomer into a polymeric network. The 3D-printed constructs showed a superior swelling capacity and improved mechanical properties as compared to pure CNCs.

A combination of melt extrusion and 3D printing was combined to produce CNC-reinforced acrylonitrile butadiene styrene (ABS) nanocomposites [84]. Lignin-coated CNCs were used for increased the thermal stability of nanocellulose that is considered beneficial during melt extrusion done at 180 °C. The extruded filament was used to 3D print nanocomposites that can have great potential in end-use products. In another study, melt processing of CNC-based nanocomposites with a hydrophobic polymeric matrix was done [40]. Polyoxyethylene (PEO) was used for this purpose that improved dispersibility and thermal stability as compared to neat CNC-based composites.

Highlight	Composition	Post-treatment	Application	References
Oxalic acid (OA) hydrolysis along with disk-milling (DM)	DM-OA-CNC: 15 (wt%)	Freeze drying	Diverse	[82]
Textured cellular architectures with modified CNCs	CNC: 0.5–40(wt%) CNC:10/20 (wt%) + HEMA + oligomer + photoinitiator	Ultraviolet curing	Building blocks	[45]

(continued)

(continued)

Highlight	Composition	Post-treatment	Application	References
CNCs aerogels	CNC: 11.8–30 (wt%) 2-CNC/Kymene (Kymene 2 wt% based on dry cellulose mass)	Freeze drying	Diverse	[58]
3D printing of melt extruded nanocomposite filaments	Lignin-coated CNCs/ABS 0–10/100–90 (wt%)	RT drying	Diverse	[84]
Gradient porosity within one scaffold	CNC/Alginate/Gelatin 70/20/10 (Dry wt%)	CaCl ₂ crosslinking	Biomedical	[44]
Surface modification of CNCs with bis(acyl)phosphane oxide (BAPO)	CNC-BAPO: 3.6 wt%	Photopolymerization	Diverse	[83]

4 Conclusions

The combination of 3D printing and cellulose nanomaterials has proved to be a successful step which is evident from the increased number of publications since last ten years (Fig. 5a) with Sweden being in top five countries (Fig. 5b). Cellulose nanofibers, crystals and bacterial cellulose suspensions are suitable for 3D printing due to its inherently suitable rheological properties. Either alone, functionalized or mixed with matrix phases, cellulose nanomaterials can be 3D printed for a variety of applications including biomedical applications, packaging, conduction devices, batteries, wearable electronic, etc. The presence of functional groups plays an important role in enhancing the efficiency and performance of cellulose nanomaterials. Either these functional groups can help in self-crosslinking of nanocellulose or they



Fig. 5 Statistics from Scopus with keywords “cellulose” and “3D Printing”. Number of publications versus **a** years and **b** countries

can also act as anchoring point for the in situ growth of other functional materials. After 3D printing of hydrogel ink, the scaffolds can be kept in wet state or are freeze-dried depending on its use and application area.

Being a biomaterial, nanocellulose has been a popular choice for biomedical applications. Furthermore, due the inherent shear thinning and anisotropy of nanocellulose, 3D printing has become a popular fabrication technique to produce nanocellulose-based scaffolds for biomedical applications [56, 85, 86]. 3D-printed scaffolds are commonly used in tissue engineering applications where interconnected porosity and controlled pore size have direct implications on their functionality both in vitro and in vivo. The clinical images can be used to design CAD files that allows the fabrication of 3D constructs that are customized for a particular patient, which reduces the rejection rate and speeds up the recovery [43].

The property of nanocellulose to form self-standing thermally stable films has been exploited for producing transparent and smooth substrates for 3D-printed electronics [87]. Nanocellulose can also be used as a matrix material for printing microfluidic devices [88].

Compared to traditional fabrication approaches, the 3D printing technology allows fabrication of complex and customized structures, in a layer-by-layer manner that improves the resolution and quality of the 3D construct. Moreover, untested geometric designs can be explored, for instance, a different directionality in each layer can be obtained as well as compositional and structural gradients are possible with multiple dispensing nozzles. In addition, living cells can be precisely positioned into specific locations of the scaffolds through 3D bioprinting.

Although rapid prototyping techniques may have several advantages, some challenges are there such as hydrogel swelling is an unavoidable feature that can reduce the resolution of the 3D-printed construct. Other challenges lie in CAD designing, slicing software and the nozzle movement. In our previous study, we have shown the importance of the nozzle movement [44]. It was observed that the using the same printing file, only a certain nozzle movement gave 3D cubic constructs with good print resolution.

References

1. Gupta V, Carrott P, Singh R, Chaudhary M, Kushwaha S (2016) Cellulose: a review as natural, modified and activated carbon adsorbent. *Bioresour Technol* 216:1066–1076
2. Moon RJ, Martini A, Nairn J, Simonsen J, Youngblood J (2011) Cellulose nanomaterials review: structure, properties and nanocomposites. *Chem Soc Rev* 40(7):3941–3994
3. Ummartyotin S, Manuspiya H (2015) A critical review on cellulose: from fundamental to an approach on sensor technology. *Renew Sustain Energy Rev* 41:402–412
4. Li M, Wu Q, Song K, Lee S, Qing Y, Wu Y (2015) Cellulose nanoparticles: Structure–morphology–rheology relationships. *ACS Sustain Chem Eng* 3(5):821–832
5. Guise C, Figueiro R (2016) Biomedical applications of nanocellulose. In: *Natural fibres: advances in science and technology towards industrial applications*. Springer, pp 155–169
6. Lin N, Dufresne A (2014) Nanocellulose in biomedicine: Current status and future prospect. *Eur Polym J* 59:302–325

7. Spence KL, Venditti RA, Rojas OJ, Habibi Y, Pawlak JJ (2011) A comparative study of energy consumption and physical properties of microfibrillated cellulose produced by different processing methods. *Cellulose* 18(4):1097–1111
8. Wang B, Sain M (2007) Dispersion of soybean stock-based nanofiber in a plastic matrix. *Polym Int.* 56(4):538–546
9. Saito T, Kimura S, Nishiyama Y, Isogai A (2007) Cellulose nanofibers prepared by TEMPO-mediated oxidation of native cellulose. *Biomacromol* 8(8):2485–2491
10. Sultan S, Abdelhamid HN, Zou X, Mathew AP (2018) CelloMOF: nanocellulose enabled 3D printing of metal–organic frameworks. *Adv Funct Mater* 1805372.
11. Chinga-Carrasco G, Ehman NV, Pettersson J et al (2018) Pulping and pretreatment affect the characteristics of bagasse inks for three-dimensional printing. *ACS Sustain Chem Eng* 6(3):4068–4075
12. Missoum K, Belgacem M, Bras J (2013) Nanofibrillated cellulose surface modification: a review. *Materials* 6(5):1745–1766
13. Henriksson M, Henriksson G, Berglund L, Lindström T (2007) An environmentally friendly method for enzyme-assisted preparation of microfibrillated cellulose (MFC) nanofibers. *Eur Polym J* 43(8):3434–3441
14. Boldizar A, Klason C, Kubat J, Näslund P, Saha P (1987) Prehydrolyzed cellulose as reinforcing filler for thermoplastics. *Int J Polym Mater* 11(4):229–262
15. Dufresne A (2013) Nanocellulose: a new ageless bionanomaterial. *Mater Today* 16(6):220–227
16. Elazzouzi-Hafraoui S, Nishiyama Y, Putaux J, Heux L, Dubreuil F, Rochas C (2007) The shape and size distribution of crystalline nanoparticles prepared by acid hydrolysis of native cellulose. *Biomacromol* 9(1):57–65
17. Iguchi M, Yamanaka S, Budhiono A (2000) Bacterial cellulose—a masterpiece of nature’s arts. *J Mater Sci* 35(2):261–270
18. Buldum G, Bismarck A, Mantalaris A (2018) Recombinant biosynthesis of bacterial cellulose in genetically modified *escherichia coli*. *Bioprocess Biosyst Eng* 41(2):265–279
19. Mishra RK, Sabu A, Tiwari SK (2018) Materials chemistry and the futurist eco-friendly applications of nanocellulose: status and prospect. *J Saudi Chem Soc* 22(8):949–978
20. Oksman K, Aitomäki Y, Mathew AP et al (2016) Review of the recent developments in cellulose nanocomposite processing. *Compos Appl Sci Manuf* 83:2–18
21. Islam MT, Alam MM, Zoccola M (2013) Review on modification of nanocellulose for application in composites. *Int J Innov Res Sci Eng Technol* 2(10):5444–5451
22. Thunberg J, Kalogeropoulos T, Kuzmenko V et al (2015) In situ synthesis of conductive polypyrrole on electrospun cellulose nanofibers: scaffold for neural tissue engineering. *Cellulose* 22(3):1459–1467
23. da Silva PM, Sierra-Avila CA, Hinestroza JP (2012) In situ synthesis of a Cu-BTC metal–organic framework (MOF 199) onto cellulosic fibrous substrates: cotton. *Cellulose* 19(5):1771–1779
24. Favier V, Cavaille J, Canova G, Shrivastava S (1997) Mechanical percolation in cellulose whisker nanocomposites. *Polym Eng Sci* 37(10):1732–1739
25. Favier V, Canova G, Cavaille J, Chanzy H, Dufresne A, Gauthier C (1995) Nanocomposite materials from latex and cellulose whiskers. *Polym Adv Technol* 6(5):351–355
26. Favier V, Chanzy H, Cavaille J (1995) Polymer nanocomposites reinforced by cellulose whiskers. *Macromolecules* 28(18):6365–6367
27. Trifol J, Plackett D, Sillard C et al (2016) A comparison of partially acetylated nanocellulose, nanocrystalline cellulose, and nanoclay as fillers for high-performance polylactide nanocomposites. *J Appl Polym Sci* 133(14)
28. Mariano M, El Kissi N, Dufresne A (2015) Melt processing of cellulose nanocrystal reinforced polycarbonate from a masterbatch process. *Eur Polym J* 69:208–223
29. Goussé C, Chanzy H, Excoffier G, Soubeyrand L, Fleury E (2002) Stable suspensions of partially silylated cellulose whiskers dispersed in organic solvents. *Polymer* 43(9):2645–2651
30. Xu W, Qin Z, Yu H et al (2013) Cellulose nanocrystals as organic nanofillers for transparent polycarbonate films. *J Nanopart Res* 15(4):1562

31. Mariano M, Dufresne A (2017) Nanocellulose: common strategies for processing of nanocomposites. *Nanocelluloses Preparation Properties Appl* 203–225
32. Gabr MH, Phong NT, Okubo K, Uzawa K, Kimpara I, Fujii T (2014) Thermal and mechanical properties of electrospun nano-cellulose reinforced epoxy nanocomposites. *Polym Test* 37:51–58
33. Naseri N, Algan C, Jacobs V, John M, Oksman K, Mathew AP (2014) Electrospun chitosan-based nanocomposite mats reinforced with chitin nanocrystals for wound dressing. *Carbohydr Polym* 109:7–15
34. Naseri N, Mathew AP, Girandon L, Fröhlich M, Oksman K (2015) Porous electrospun nanocomposite mats based on chitosan–cellulose nanocrystals for wound dressing: Effect of surface characteristics of nanocrystals. *Cellulose* 22(1):521–534
35. Svagan AJ, Jensen P, Dvinskikh SV, Furó I, Berglund LA (2010) Towards tailored hierarchical structures in cellulose nanocomposite biofoams prepared by freezing/freeze-drying. *J Mater Chem* 20(32):6646–6654
36. Naseri N, Poirier J, Girandon L, Fröhlich M, Oksman K, Mathew AP (2016) 3-dimensional porous nanocomposite scaffolds based on cellulose nanofibers for cartilage tissue engineering: Tailoring of porosity and mechanical performance. *R Soc Chem Adv* 6(8):5999–6007
37. Karim Z, Mathew AP, Grahn M, Mouzon J, Oksman K (2014) Nanoporous membranes with cellulose nanocrystals as functional entity in chitosan: Removal of dyes from water. *Carbohydr Polym* 112:668–676
38. Oksman K, Mathew AP, Bondeson D, Kvien I (2006) Manufacturing process of cellulose whiskers/poly(lactic acid) nanocomposites. *Compos Sci Technol* 66(15):2776–2784
39. De Menezes AJ, Siqueira G, Curvelo AA, Dufresne A (2009) Extrusion and characterization of functionalized cellulose whiskers reinforced polyethylene nanocomposites. *Polymer* 50(19):4552–4563
40. Ben Azouz K, Ramires EC, Van den Fonteyne W, El Kissi N, Dufresne A (2011) Simple method for the melt extrusion of a cellulose nanocrystal reinforced hydrophobic polymer. *ACS Macro Lett* 1(1):236–240
41. Gebhardt A (2012) Understanding additive manufacturing: rapid prototyping-rapid tooling-rapid manufacturing. Carl Hanser Verlag GmbH Co KG
42. Ambrosi A, Pumera M (2016) 3D-printing technologies for electrochemical applications. *Chem Soc Rev* 45(10):2740–2755
43. Bücking TM, Hill ER, Robertson JL, Maneas E, Plumb AA, Nikitichev DI (2017) From medical imaging data to 3D printed anatomical models. *PLoS ONE* 12(5):e0178540
44. Sultan S, Mathew AP (2018) 3D printed scaffolds with gradient porosity based on a cellulose nanocrystal hydrogel. *Nanoscale* 10:4421–4431
45. Siqueira G, Kokkinis D, Libanori R et al (2017) Cellulose nanocrystal inks for 3D printing of textured cellular architectures. *Adv Func Mater* 27(12):1604619–1604629
46. Compton BG, Lewis JA (2014) 3D-printing of lightweight cellular composites. *Adv Mater* 26(34):5930–5935
47. Studart AR (2016) Additive manufacturing of biologically-inspired materials. *Chem Soc Rev* 45(2):359–376
48. Zhu N, Chen X (2013) Biofabrication of tissue scaffolds. In: *Advances in biomaterials science and biomedical applications*. InTech
49. Lee JM, Yeong WY (2016) Design and printing strategies in 3D bioprinting of cell-hydrogels: a review. *Advanced healthcare materials*
50. Chung JH, Naficy S, Yue Z et al (2013) Bio-ink properties and printability for extrusion printing living cells. *Biomater Sci* 1(7):763–773
51. Chang R, Nam J, Sun W (2008) Effects of dispensing pressure and nozzle diameter on cell survival from solid freeform fabrication–based direct cell writing. *Tissue Eng Part* 14(1):41–48
52. Moberg T, Sahlin K, Yao K et al (2017) Rheological properties of nanocellulose suspensions: effects of fibril/particle dimensions and surface characteristics. *Cellulose* 24(6):2499–2510
53. Shin S, Park S, Park M et al (2017) Cellulose nanofibers for the enhancement of printability of low viscosity gelatin derivatives. *BioResources* 12(2):2941–2954

54. Lasseguette E, Roux D, Nishiyama Y (2008) Rheological properties of microfibrillar suspension of TEMPO-oxidized pulp. *Cellulose* 15(3):425–433
55. Gladman AS, Matsumoto EA, Nuzzo RG, Mahadevan L, Lewis JA (2016) Biomimetic 4D printing. *Nat Mater* 15:413–418
56. Chinga-Carrasco G (2018) Potential and limitations of nanocelluloses as components in biocomposite inks for three-dimensional bioprinting and for biomedical devices. *Biomacromol* 19(3):701–711
57. Wang J, Chiappone A, Roppolo I et al (2018) All-in-One cellulose nanocrystals for 3D printing of nanocomposite hydrogels. *Angew Chem Int Ed* 57(9):2353–2356
58. Li VC, Dunn CK, Zhang Z, Deng Y, Qi HJ (2017) Direct ink write (DIW) 3D printed cellulose nanocrystal aerogel structures. *Sci Rep* 7(1):8018–8026
59. Lee KY, Mooney DJ (2012) Alginate: properties and biomedical applications. *Prog Polym Sci* 37(1):106–126
60. Duan B, Hockaday LA, Kang KH, Butcher JT (2013) 3D bioprinting of heterogeneous aortic valve conduits with alginate/gelatin hydrogels. *J Biomed Mater Res, Part 101(5)*:1255–1264
61. Mertaniemi H, Escobedo-Lucea C, Sanz-Garcia A et al (2016) Human stem cell decorated nanocellulose threads for biomedical applications. *Biomaterials* 82:208–220
62. Ávila HM, Schwarz S, Rotter N, Gatenholm P (2016) 3D bioprinting of human chondrocyte-laden nanocellulose hydrogels for patient-specific auricular cartilage regeneration. *Bioprinting* 1:22–35
63. Henriksson I, Gatenholm P, Hägg D (2017) Increased lipid accumulation and adipogenic gene expression of adipocytes in 3D bioprinted nanocellulose scaffolds. *Biofabrication* 9(1):015022
64. Moller T, Amoroso M, Hagg D et al (2017) In vivo chondrogenesis in 3D bioprinted human cell-laden hydrogel constructs. *Plast Reconstr Surg Glob Open* 5(2):e1227
65. Markstedt K, Mantas A, Tournier I, Martínez Ávila H, Hägg D, Gatenholm P (2015) 3D bioprinting human chondrocytes with nanocellulose–alginate bioink for cartilage tissue engineering applications. *Biomacromol* 16(5):1489–1496
66. Håkansson KM, Henriksson IC, de la Peña Vázquez, Cristina et al (2016) Solidification of 3D printed nanofibril hydrogels into functional 3D cellulose structures. *Adv Mater Technol* 1(7):1600096
67. Rees A, Powell LC, Chinga-Carrasco G et al (2015) 3D bioprinting of carboxymethylated-periodate oxidized nanocellulose constructs for wound dressing applications. *Biomed Res Int* 2015(2015):925757–925764
68. Nguyen D, Hägg DA, Forsman A et al (2017) Cartilage tissue engineering by the 3D bioprinting of iPS cells in a nanocellulose/alginate bioink. *Sci Rep* 7(1):658
69. Müller M, Öztürk E, Arlov Ø, Gatenholm P, Zenobi-Wong M (2017) Alginate sulfate–nanocellulose bioinks for cartilage bioprinting applications. *Ann Biomed Eng* 45(1):210–223
70. Markstedt K, Escalante A, Toriz G, Gatenholm P (2017) Biomimetic inks based on cellulose nanofibrils and cross-linkable xylans for 3D printing. *ACS Appl Mater Interfaces* 9(46):40878–40886
71. Leppiniemi J, Lahtinen P, Paajanen A et al (2017) 3D-printable bioactivated nanocellulose–Alginate hydrogels. *ACS Appl Mater Interfaces* 9(26):21959–21970
72. Guillermo J, De L (2016) Cellulose nanofibril hydrogel tubes as sacrificial templates for freestanding tubular cell constructs. *Biomacromol* 17(3):905–913
73. Li Y, Zhu H, Wang Y et al (2017) Cellulose–Nanofiber–Enabled 3D printing of a carbon–nanotube microfiber network. *Small Methods* 1(10):1700222
74. Shao Y, Chaussy D, Grosseau P, Beneventi D (2015) Use of microfibrillated cellulose/lignosulfonate blends as carbon precursors: Impact of hydrogel rheology on 3D printing. *Ind Eng Chem Res* 54(43):10575–10582
75. Li VC, Mulyadi A, Dunn CK, Deng Y, Qi HJ (2018) Direct ink write 3D printed cellulose nanofiber aerogel structures with highly deformable, shape recoverable, and functionalizable properties. *ACS Sustain Chem Eng* 6(2):2011–2022
76. Wang B, Benitez AJ, Lossada F, Merindol R, Walther A (2016) Bioinspired mechanical gradients in cellulose nanofibril/polymer nanopapers. *Angew Chem* 128(20):6070–6074

77. Dong J, Li M, Zhou L et al (2017) The influence of grafted cellulose nanofibers and postextrusion annealing treatment on selected properties of poly (lactic acid) filaments for 3D printing. *J Polym Sci Part B Polym Phys* 55(11):847–855
78. Wang L, Gardner DJ, Bousfield DW (2018) Cellulose nanofibril-reinforced polypropylene composites for material extrusion: Rheological properties. *Polym Eng Sci* 58(5):793–801
79. Markstedt K, Sundberg J, Gatenholm P (2014) 3D bioprinting of cellulose structures from an ionic liquid. *3D Printing Addit Manuf* 1(3):115–121
80. Schaffner M, Rühls PA, Coulter F, Kilcher S, Studart AR (2017) 3D printing of bacteria into functional complex materials. *Sci Adv* 3(12):eaao6804
81. Lehner BA, Schmieden DT, Meyer AS (2017) A straightforward approach for 3D bacterial printing. *ACS Synth Biol* 6(7):1124–1130
82. Jia C, Bian H, Gao T et al (2017) Thermally stable cellulose nanocrystals toward high-performance 2D and 3D nanostructures. *ACS Appl Mater Interfaces* 9(34):28922–28929
83. Wang J, Chiappone A, Roppolo I et al (2018) All-in-one cellulose nanocrystals for 3D printing of nanocomposite hydrogels. *Angew Chem Int Edn.* 57(9):2353–2356
84. Feng X, Yang Z, Rostom SS, Dadmun M, Xie Y, Wang S (2017) Structural, mechanical, and thermal properties of 3D printed L-CNC/acrylonitrile butadiene styrene nanocomposites. *J Appl Polym Sci* 134(31):45082
85. Sultan S, Siqueira G, Zimmermann T, Mathew AP (2017) 3D printing of nano-cellulosic biomaterials for medical applications. *Curr Opin Biomed Eng* 2:29–34
86. Xu W, Wang X, Sandler N, Willför S, Xu C (2018) Three-dimensional printing of wood-derived biopolymers: a review focused on biomedical applications. *ACS Sustain Chem Eng* 6(5):5663–5680
87. Hoeng F, Denneulin A, Bras J (2016) Use of nanocellulose in printed electronics: a review. *Nanoscale* 8(27):13131–13154
88. Shin S, Hyun J (2017) Matrix-assisted three-dimensional printing of cellulose nanofibers for paper microfluidics. *ACS Appl Mater Interfaces* 9(31):26438–26446